Mechanical stretch increases Kv1.5 current through an interaction between the S1–S2 linker and N-terminus of the channel

Received for publication, September 30, 2019, and in revised form, February 27, 2020 Published, Papers in Press, March 2, 2020, DOI 10.1074/jbc.RA119.011302

Alexandria O. Milton, Tingzhong Wang, Wentao Li, Jun Guo, and Shetuan Zhang

From the Department of Biomedical and Molecular Sciences, Queen's University, Kingston, ON K7L 3N6, Canada

Edited by Mike Shipston

The voltage-gated potassium channel Kv1.5 plays important roles in atrial repolarization and regulation of vascular tone. In the present study, we investigated the effects of mechanical stretch on Kv1.5 channels. We induced mechanical stretch by centrifuging or culturing Kv1.5-expressing HEK 293 cells and neonatal rat ventricular myocytes in low osmolarity (LO) medium and then recorded Kv1.5 current ($I_{Kv1.5}$) in a normal, isotonic solution. We observed that mechanical stretch increased $I_{Kv1.5}$, and this increase required the intact, long, proline-rich extracellular S1–S2 linker of the Kv1.5 channel. The low osmolarity–induced $I_{Kv1.5}$ increase also required an intact intracellular N terminus, which contains the binding motif for endogenous Src tyrosine kinase that constitutively inhibits $I_{Kv1.5}$. Disrupting the Src-binding motif of Kv1.5 through N-terminal truncation or mutagenesis abolished the mechanical stretch-mediated increase in $I_{Kv1.5}$. Our results further showed that the extracellular S1–S2 linker of Kv1.5 communicates with the intracellular N terminus. Although the S1–S2 linker of WT Kv1.5 could be cleaved by extracellularly applied proteinase K (PK), an N-terminal truncation up to amino acid residue 209 altered the conformation of the S1–S2 linker and made it no longer susceptible to proteinase K–mediated cleavage. In summary, the findings of our study indicate that the S1–S2 linker of Kv1.5 represents a mechanosensor that regulates the activity of this channel. By targeting the S1–S2 linker, mechanical stretch may induce a change in the N-terminal conformation of Kv1.5 that relieves Src-mediated tonic channel inhibition and results in an increase in $I_{Kv1.5}$.

The voltage-gated potassium channel Kv1.5 mediates the ultra-rapid delayed rectifier potassium current (I_{Kur})[2] in atrial myocytes (1), which is critical for atrial repolarization (2). Kv1.5 also contributes to the regulation of vascular smooth muscle tone (3, 4). The Kv1.5 channel is composed of four α-subunits; each subunit contains six transmembrane segments and cytoplasmic N and C termini. The extracellularly localized S1–S2 linker of Kv1.5 is unusually long, containing 54 amino acid residues compared with 5–44 amino acid residues for most other Kv channels (UniProt: P22460). We have previously demonstrated that extracellularly applied proteinase K (PK) cleaves Kv1.5 channels at a single site in the S1–S2 linker, separating the channel into an N-fragment (N terminus to S1) and a C-fragment (S2 to C terminus) (5). The N-fragments of Kv1.5 were found to interact with the rest of the channel to accomplish specific tasks related to channel function (6).

Dysfunction of I_{Kur} has been linked to atrial fibrillation, an arrhythmia prevalent in the elderly and patients with chronic heart failure (7–9). Atrial fibrillation also develops from pathological conditions such as heart failure, hypertension, and dilated cardiomyopathy, conditions which involve myocardial stretch (10–12).

Cardiomyocytes are exposed to mechanical forces, including stretch, compression, and shear. Alterations of mechanical forces may modify cardiomyocyte electrical, mechanical, metabolic, and structural properties. In this regard, mechano-gated ion channels have been identified as cardiac mechanoreceptors solely activated by a mechanical stimulus. They convert mechanical stimuli into electrical and biochemical signals, regulating various cellular processes in response to extracellular mechanical forces (13). In addition, some ion channels that are activated by nonmechanical stimuli can be mechanically modulated, leading to altered channel activity (13). In this regard, the voltage-gated Kv1.5 channel has been shown to be regulated by mechanical stretch. Guo *et al.* (14) reported that application of mechanical force by 48-h cyclic stretch at 0.5 Hz with 20% elongation in length increases voltage-gated Kv1.5 channel expression by 48% in cultured neonatal rat ventricular myocytes. Boycott *et al.* (15) found that the Kv1.5 channel is modulated by shear stress through mechanically induced redistribution of intracellular Kv1.5 into the sarcolemma of rat atrial myocytes. Nonetheless, the molecular mechanisms underlying the effects of mechanical force on Kv1.5 channel activity are not well-understood. In the present study, we demonstrate that mechanical stretch mediated by cell swelling and centrifugation increases Kv1.5 current ($I_{Kv1.5}$). We show that the S1–S2 linker may serve as a mechanosensor, mediating stretch-induced increase in $I_{Kv1.5}$ because of enhanced channel density in the plasma membrane through altered Src-interaction with the N terminus of the channel.

This work was supported by Natural Sciences and Engineering Research Council of Canada Grant RGPIN-2019-04878 (to S. Z.). The authors declare that they have no conflicts of interest with the contents of this article.

[1] To whom correspondence should be addressed: 18 Stuart Street, Kingston, Ontario K7L 3N6, Canada. Tel.: 613-533-3348; Fax: 613-533-6412; E-mail: shetuan.zhang@queensu.ca.

[2] The abbreviations used are: I_{Kur}, ultra-rapidly activating delayed rectifier potassium current; PK, proteinase K; $I_{Kv1.5}$, Kv1.5 current; Kv1.5-HEK, Kv1.5-expressing HEK cells; LO, low extracellular osmolarity; MEM, minimum essential medium; CTL, control; Kv, voltage-gated potassium; $V_{1/2}$, voltage of half-maximal activation.

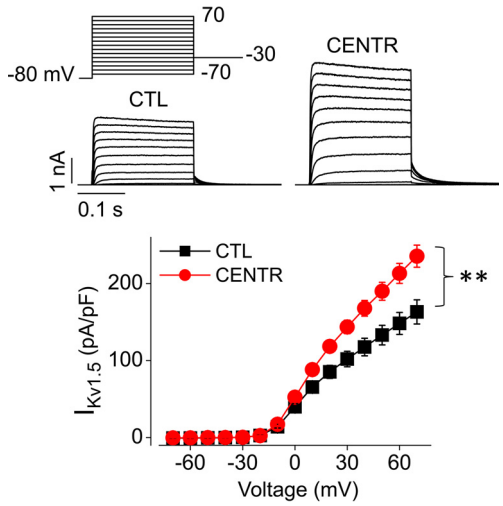

Figure 1. Centrifugation increases $I_{Kv1.5}$. Kv1.5-HEK cells were centrifuged (*CENTR*) at 70 × *g* for 5 min. Cells were then re-suspended in normal culture medium for 20 min prior to $I_{Kv1.5}$ recordings. Kv1.5-HEK cells without centrifugation were used as control (CTL). Representative current traces along with the voltage protocol (*top*) and summarized I-V relationship (*bottom*) are shown. CTL, $n = 29$; CENTR, $n = 38$; **, $p < 0.01$ at 20 mV and above.

Results

Mechanical stretch by centrifugation increases $I_{Kv1.5}$

During an experiment that involved centrifuging Kv1.5-expressing HEK (Kv1.5-HEK) cells, we unexpectedly discovered that centrifugation caused an increase in $I_{Kv1.5}$. We centrifuged Kv1.5-HEK cells at 70 × *g* for 5 min, and then suspended cells in minimum essential medium (MEM) for 20 min prior to whole-cell voltage clamp recordings. The centrifugation led to an increase in $I_{Kv1.5}$ compared with control (CTL, without centrifugation) (Fig. 1). Because relatively low-speed centrifugation allows Kv1.5-HEK cells to experience mechanical stretch from gravitational-force accelerations, this result suggests that channel activity is altered by mechanical force.

LO treatment increases $I_{Kv1.5}$

To further evaluate the effect of mechanical stretch on Kv1.5 activity, the osmotic potential of the cell culture medium was altered to induce cell swelling (16–18). Specifically, standard MEM cell culture medium was mixed with purified distilled water at a 2:1 ratio, thus decreasing the osmolarity from 315 to 211 mOsm/liter (33% reduction). The degree of membrane stretch was examined using live cell imaging of Kv1.5-HEK cells cultured in isotonic (CTL) or hypotonic (LO) medium. Kv1.5-HEK cell size increased significantly after 30-min treatment with LO culture medium compared with control (Fig. 2*A*).

To examine the LO treatment on $I_{Kv1.5}$, Kv1.5-HEK cells were cultured in LO medium for various periods. The cells were then transferred to a perfusion chamber bathed with isotonic Tyrode solution, and $I_{Kv1.5}$ was recorded. LO-induced $I_{Kv1.5}$ increase occurred after 10 min (data not shown), reached maximum at 30 min (Fig. 2*B*), and did not develop further at 60 min (data not shown). The LO-induced increase in $I_{Kv1.5}$ at 30 min was not associated with a change in the activation curve (Fig. 2*B*, *bottom right*). The voltages of half-maximal activation ($V_{1/2}$) were −7.6 ± 0.7 mV for control and −7.7 ± 0.7 mV for LO ($p > 0.05$). The slope factors were 6.1 ± 0.2 for control and 6.6 ± 0.2 for LO ($p > 0.05$).

To examine whether LO increased $I_{Kv1.5}$ can recover upon re-culture in normal (isotonic) medium, we cultured multiple plates of Kv1.5-HEK cells in LO medium for 30 min. The culture media were then changed to normal (isotonic) medium. After various periods of culture, cells were collected and $I_{Kv1.5}$ was recorded. LO-induced $I_{Kv1.5}$ increase was reversible; The increased $I_{Kv1.5}$ was significantly recovered after 2 h and returned to control level after 4 h of re-culturing cells in normal medium (Fig. 2*C*).

To determine whether the mechanical stretch-induced increase in $I_{Kv1.5}$ also occurs in native cardiac myocytes, we studied Kv1.5 channels expressed in neonatal rat ventricular myocytes. The endogenous Kv1.5 current in cardiac myocytes is small and complicated by the coexistence of other K^+ channels. To overcome this issue, we transfected neonatal rat ventricular myocytes cultured on glass coverslips with human Kv1.5 plasmid. Twenty-four h after transfection, we treated the myocytes with LO media for 30 min. The cells were then transferred to the recording chamber and currents were recorded in isotonic Tyrode solution. As shown in Fig. 3, LO treatment for 30 min also significantly increased $I_{Kv1.5}$ in neonatal rat ventricular myocytes.

LO treatment–mediated current increase is specific to Kv1.5

To determine whether LO treatment–mediated current increase observed in Kv1.5 also exists in other Kv channels, we treated HEK cells stably expressing Kv1.4, Kv4.3, Kv7.1+KCNE1, Kv10.1, or Kv11.1, respectively, with LO medium in culture for 30 min. After treatment, various currents were recorded in normal isotonic Tyrode solution. Although LO treatment slightly and nonsignificantly increased $I_{Kv4.3}$, it did not affect $I_{Kv1.4}$, $I_{Kv7.1+KCNE1}$, $I_{Kv10.1}$, or $I_{Kv11.1}$ (Fig. 4). Thus, LO treatment selectively increased $I_{Kv1.5}$.

The S1–S2 linker of Kv1.5 is involved in LO-induced current increase

Compared with other Kv channels, the extracellular S1–S2 linker of the Kv1.5 channel is long and proline-rich, and uniquely contains an *N*-linked glycosylation site (Fig. 5*A*). To investigate whether the S1–S2 linker is involved in the mechanical stretch-induced increase in $I_{Kv1.5}$, we used the following strategies.

First, we examined whether an intact S1–S2 linker is required for LO-meditated $I_{Kv1.5}$ increase. We previously demonstrated that extracellularly applied PK precisely cleaves cell-surface Kv1.5 proteins at a single site in the S1–S2 linker, separating the 75-kDa channel protein into a 42-kDa N-fragment and a 33-kDa C-fragment (5, 6). In the present study, we pretreated Kv1.5-HEK cells with PK (200 μg/ml, 20 min) and cultured cells in LO or normal (control) medium for 30 min. Cells were then transferred to the perfusion chamber to record $I_{Kv1.5}$ in isotonic Tyrode bath solution. PK pretreatment prevented the LO-mediated increase in $I_{Kv1.5}$, indicating that an intact S1–S2 linker is necessary for LO-mediated effect (Fig. 5*B*).

Second, proline residues play important structural and functional roles for channel activity (19–22). The Kv1.5 channel uniquely possesses 12 proline residues in the S1–S2 linker. To characterize the functional importance of these residues in the LO-mediated $I_{Kv1.5}$ increase, we created a mutant Kv1.5 chan-

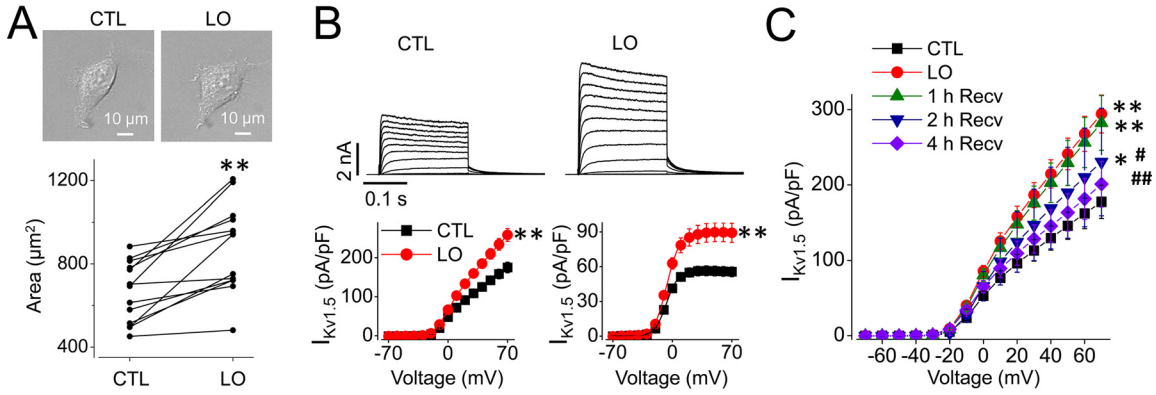

Figure 2. LO medium treatment increases cell size and reversibly increases $I_{Kv1.5}$. *A,* culture of Kv1.5-HEK cells with LO medium for 30 min increased cell size ($n = 13$; **, $p < 0.01$). *B,* culture of Kv1.5-HEK cells with LO medium for 30 min increased $I_{Kv1.5}$. Representative current traces are depicted above the summarized I-V relationships (*left*) and activation curves (*right*). Activation curves were fitted to the Boltzmann function to determine $V_{1/2}$ values and slope factors. CTL, $n = 47$; LO, $n = 31$; **, $p < 0.01$ at 20 mV and above for I-V curves; and tail currents at −30 mV following 50 mV depolarization for activation curves. *C,* LO-treatment mediated increase in $I_{Kv1.5}$ recovered (*Recv*) with time upon re-culture of cells in normal (isotonic) medium. Summarized I-V relationships at various time points were obtained from 7–27 cells. *, $p < 0.05$; **, $p < 0.01$ *versus* CTL at 20 mV and above; #, $p < 0.05$; ##, $p < 0.01$ *versus* LO at 20 mV and above.

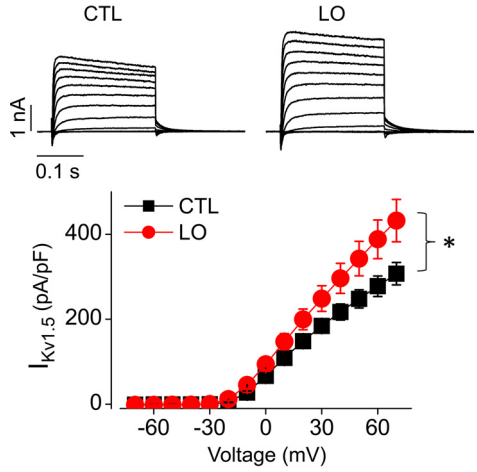

Figure 3. LO medium treatment increases $I_{Kv1.5}$ in neonatal rat ventricular myocytes transfected with Kv1.5. Representative current traces are depicted above the summarized I-V relationship. CTL, $n = 32$; LO, $n = 32$. *, $p < 0.05$ at 20 mV and above.

nel, Kv1.5–12PA, in which all 12 nonconserved prolines (P) are replaced with alanines (A). LO treatment failed to affect Kv1.5–12PA current (Fig. 5*C*). Furthermore, we created another mutant Kv1.5 channel, Kv1.5-Δ282–300, in which amino acid residues from 282 to 300 in the S1–S2 linker were deleted. This led to removal of seven nonconserved prolines in the S1–S2 linker. Kv1.5-Δ282–300 current was also unaffected by LO treatment (Fig. 5*D*). Thus, an intact S1–S2 linker containing the nonconserved proline residues plays a role in the mechanical stretch-induced effect on Kv1.5 channel function.

Third, Kv1.5 channels are glycosylated and *N*-linked glycosylation occurs at a site (Asn-299) located in the S1–S2 linker (5). To investigate the role of glycosylation in LO-mediated increase in $I_{Kv1.5}$, we treated Kv1.5-HEK cells with tunicamycin (10 μg/ml) for 36 h, which led to a complete inhibition of *N*-glycosylation, as reported previously (5, 6). LO treatment failed to affect $I_{Kv1.5}$ of channels treated with tunicamycin (Fig. 5*E*). Thus, glycosylation at a site in the S1–S2 linker plays an important role in LO-mediated Kv1.5 increase.

The Kv1.5 channel N terminus is involved in the LO-mediated $I_{Kv1.5}$ increase

The N terminus of Kv1.5 is an important target region for channel regulation. To investigate the involvement of the intracellular N terminus of the Kv1.5 channel in the LO-mediated effect, we deleted residues 1–209 of the N terminus, creating the ΔN209 mutant Kv1.5 channel, which was stably expressed in HEK293 (ΔN209 Kv1.5-HEK) cells. Truncation of the N terminus abolished LO-mediated current increase seen in WT Kv1.5 channels (Fig. 6, *A* and *B*). Thus, the N terminus of Kv1.5 plays a role in the LO-mediated increase in $I_{Kv1.5}$.

In contrast to Kv1.5, Kv1.4 was insensitive to LO treatment (Fig. 6*C*), and has a different N-terminal amino acid sequence (Fig. 6*E*). To validate the role of the Kv1.5 N terminus in LO-mediated increase in $I_{Kv1.5}$, we created a mutant Kv1.5 channel Kv1.5–Kv1.4NT, in which the N terminus of Kv1.5 is replaced with that of Kv1.4. The LO-mediated increase in $I_{Kv1.5}$ seen in WT Kv1.5 channels was not observed in the Kv1.5–Kv1.4NT mutant channel (Fig. 6, *A* and *D*). This result further confirms the importance of the Kv1.5 N terminus in LO-induced increase in $I_{Kv1.5}$.

Disruption of Src-binding sites abolishes LO-induced increase in $I_{Kv1.5}$

It has been shown that Src tyrosine kinase interacts with Kv1.5, leading to an inhibition of $I_{Kv1.5}$ (23). The Src homology 3 (SH3) domain of Src binds to the proline-rich motif RPLPXXP in partner proteins (24). The N terminus between amino acid residues 65 and 82 of Kv1.5 contains two repeats of the SH3 domain–binding motif RPLPPLP (23). However, Kv1.4 does not contain such a motif (Fig. 6*E*). To examine whether Src-mediated regulation of the Kv1.5 channel is involved in LO-induced increase in $I_{Kv1.5}$, we disrupted Src-channel interaction by deleting the Src-binding motifs from the Kv1.5 channel. Specifically, we deleted amino acids 64–82 of the Kv1.5 channel, creating Kv1.5-ΔPro (Kv1.5 with deletion of proline-rich Src-binding domains, Fig. 7*A*). Unlike WT Kv1.5 channels (Fig. 7*B*), Kv1.5-ΔPro mutant channels were unaffected by LO treatment (Fig. 7*C*).

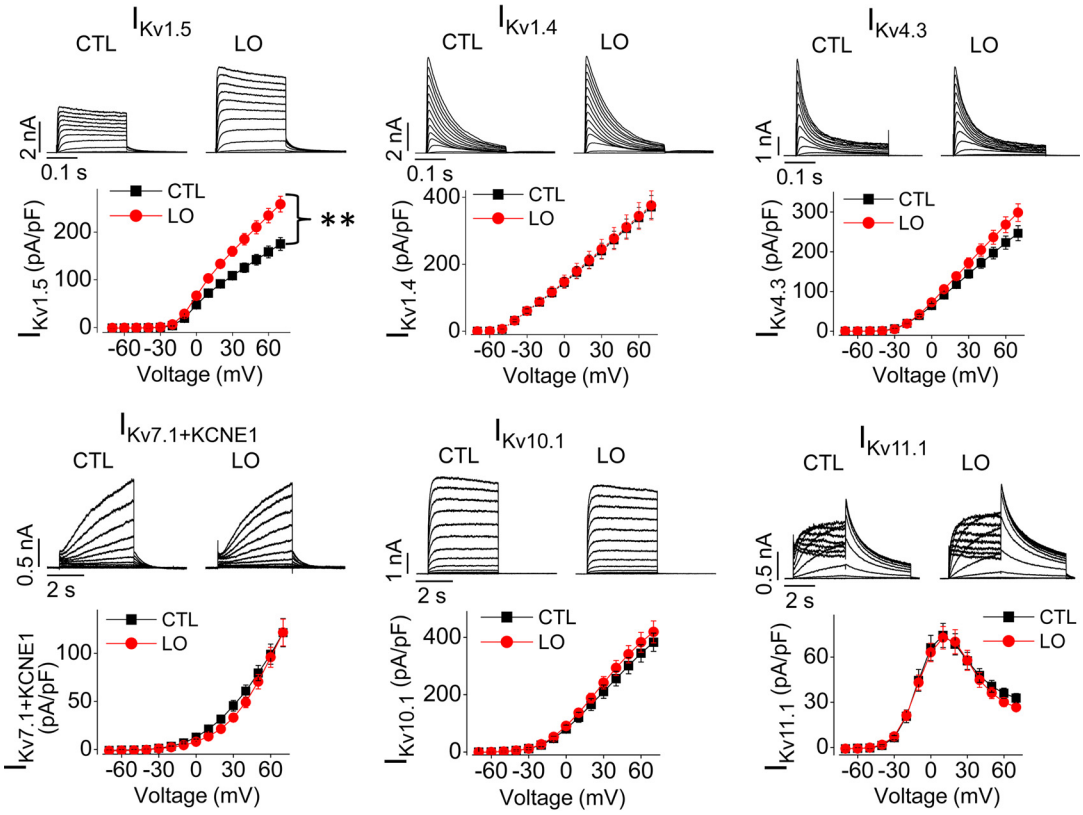

Figure 4. Mechanical stretch induced by LO medium culture selectively increases $I_{Kv1.5}$. Currents from Kv1.5, Kv1.4, Kv4.3, Kv7.1+KCNE1, Kv10.1, and Kv11.1 channels were recorded from HEK 293 cells stably expressing the respective channels in control cells and cells treated with LO medium for 30 min. Representative current traces are depicted above the summarized I-V relationships. For $I_{Kv1.5}$, CTL, $n = 47$; LO, $n = 31$ (same set of data shown in Fig. 2*B*). For $I_{Kv1.4}$, CTL, $n = 43$; LO, $n = 46$; for $I_{Kv4.3}$, CTL, $n = 42$; LO, $n = 42$; for $I_{Kv7.1+KCNE1}$, CTL, $n = 15$; LO, $n = 12$; for $I_{Kv10.1}$, CTL, $n = 18$, LO, $n = 18$; for $I_{Kv11.1}$, CTL, $n = 23$, LO, $n = 19$. **, $p < 0.01$ at 20 mV and above.

Cells such as HEK 293 cells and native cardiac myocytes express endogenous Src (23, 25, 26). We believe that Kv1.5 channels are under tonic inhibition by Src kinases. LO treatment may cause a relief of such tonic inhibition, leading to an increase in $I_{Kv1.5}$. To this end, we examined the effects of Src kinase inhibitor PP1 (27) and LO treatment on the expression and function of Kv1.5 channels. On Western blot analysis, Kv1.5 channels from whole-cell lysate display as a 68-kDa and a 75-kDa band (5, 6). The former represents the core-glycosylated immature protein inside the cell, and the latter represents the fully glycosylated mature protein normally localized in the plasma membrane (5). Our results revealed that neither LO treatment (30 min) nor PP1 treatment (10 μM, 1 h) affected the total amount of mature (75-kDa) channel expression in whole cell lysate (Fig. 8, *A* and *B*, *left lanes*). It has been reported that mechanical stretch leads to redistribution of Kv1.5 channels toward the plasma membrane (15). To address this possibility, we isolated cell surface protein using biotinylation (5). LO treatment as well as PP1 treatment increased the density of cell-surface 75-kDa channels (Fig. 8, *A* and *B*, *right lanes*). Indeed, incubation of Kv1.5-HEK cells with Src inhibitor PP1 (10 μM) for 1 h led to an increase in $I_{Kv1.5}$, similar to the LO-mediated $I_{Kv1.5}$ increase (Fig. 8*C*). Furthermore, after pretreatment with Src inhibitor PP1, LO treatment no longer increased $I_{Kv1.5}$ (Fig. 8*C*). These results suggest that LO increases $I_{Kv1.5}$ by disrupting Src interaction with the channel, which leads to accumulation of Kv1.5 channels on the plasma membrane.

The Kv1.5 S1–S2 linker communicates with the N terminus

Our data so far indicate that both the S1–S2 linker and the N terminus are involved in the mechanical stretch-mediated increase in $I_{Kv1.5}$. We propose that mechanical stretch increases membrane channel density and $I_{Kv1.5}$ through a conformational change in the N terminus mediated via the S1–S2 linker, which releases Src-channel interaction. To test this notion, we examined the communication between the S1–S2 linker and N terminus.

To investigate whether the extracellular S1–S2 linker conformation can be affected by a modified N terminus, we used the N-terminal truncation channel ΔN209 that is functional (Fig. 6*B*). Compared with WT channel proteins, Kv1.5 ΔN209 has a smaller molecular mass. Western blot analysis of ΔN209 displays a 50-kDa band, representing the mature channel protein, and a 45-kDa band, representing the immature protein. We have previously demonstrated that extracellularly applied PK (200 μg/ml, 20 min) cleaves the 75-kDa protein of WT channels at a site in the S1–S2 linker, generating an N-fragment and a C-fragment (5, 6). Consistently, PK treatment selectively cleaved the cell-surface 75-kDa band (without affecting the intracellularly localized 68-kDa band), generating a 33-kDa band detected with a C-terminal antibody (Fig. 9*A*). However, despite the fact that the 50-kDa ΔN209 protein is also located in the cell-surface to generate current, PK treatment could not cleave it (Fig. 9*B*). Thus, shortening of the intracellular N ter-

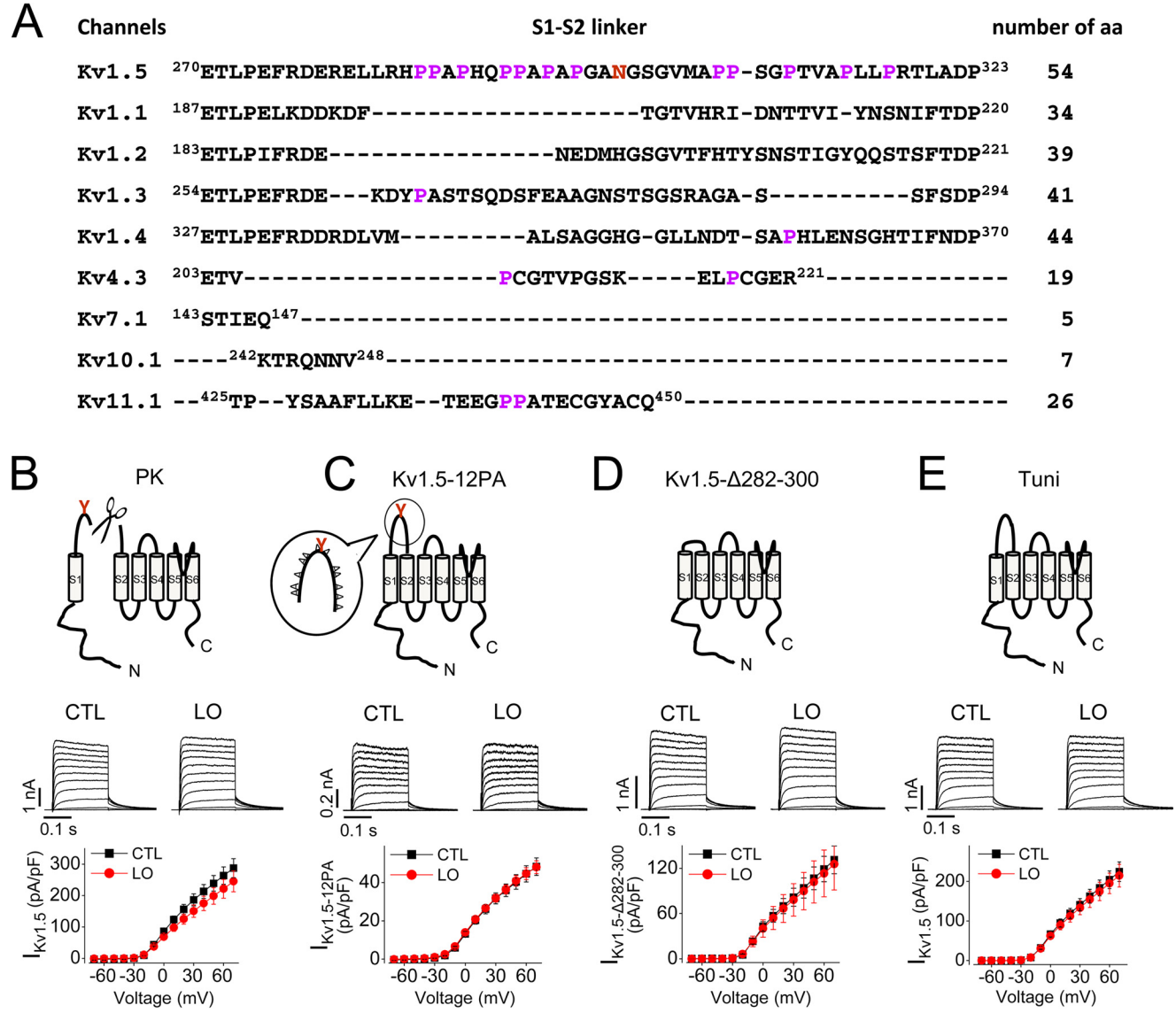

Figure 5. The unique S1–S2 linker of Kv1.5 is involved in LO-mediated increase in $I_{Kv1.5}$. *A*, amino acid sequences of the S1–S2 linker of various Kv channels. Kv1.5 possesses an unusually long S1–S2 linker with 12 nonconserved proline residues (in *magenta*). The *N*-linked glycosylation site is shown in *red*. *B,* PK cleavage of the S1–S2 linker abolished LO-induced increase in $I_{Kv1.5}$. Schematic illustration of Kv1.5 PK cleavage (*top*) and representative current traces (*middle*) are depicted above the summarized I-V relationships (*bottom*). CTL, $n = 14$; LO, $n = 21$. *C,* mutating all 12 nonconserved prolines (P) to alanines (A) in the S1–S2 linker abolished LO-induced increase in $I_{Kv1.5}$. Schematic illustration of the Kv1.5–12PA mutant (*top*) as well as representative current traces (*middle*) are depicted above the summarized I-V relationships (*bottom*). CTL, $n = 37$; LO, $n = 36$. *D*, deletion of amino acid residues 282–300 in the S1–S2 linker abolished LO-induced increase in $I_{Kv1.5}$. Schematic illustration of Kv1.5-Δ282–300 mutant (*top*) as well as representative current traces (*middle*) are depicted above the summarized I-V relationships (*bottom*). CTL, $n = 15$, LO, $n = 10$. *E*, inhibition of glycosylation in the S1–S2 linker with tunicamycin (*Tuni*) treatment abolished the LO-induced increase in $I_{Kv1.5}$. Schematic illustration of WT Kv1.5 without glycosylation (*top*) as well as representative current traces (*middle*) are depicted above the summarized I-V relationships (*bottom*). CTL, $n = 24$; LO, $n = 24$.

minus causes a conformational change in the extracellular S1–S2 linker of the channel, making the linker resistant to cleavage by PK (Fig. 9). These data provide direct evidence that the S1–S2 linker communicates with the N terminus in a conformational manner.

Discussion

Although ion channels can be activated by a single primary stimulus, some are polymodal and can be activated by multiple types of stimuli such as voltage and temperature (28). Because Kv1.5-expressing atrial myocytes and vascular smooth muscle cells are exposed to mechanical forces that may change in various conditions, investigating the role of mechanical force on Kv1.5 is an important step toward understanding the regulation and role of this channel in pathophysiological conditions.

Our results revealed that $I_{Kv1.5}$ was increased by centrifugation (Fig. 1) and LO treatment (Figs. 2 and 3), and LO-mediated current increase was specific to the Kv1.5 channel among Kv channels tested in the present study (Fig. 4). Centrifugation exerts gravitational force on cells causing membrane stretch against the interior of the centrifugation tube, leading to an increase in $I_{Kv1.5}$. Membrane stretch induced by hypotonic solution is an established strategy to study the effect of mechanical force on ion channels (29–31). In our study, Kv1.5-HEK cells were cultured with LO media for 30 min, then currents

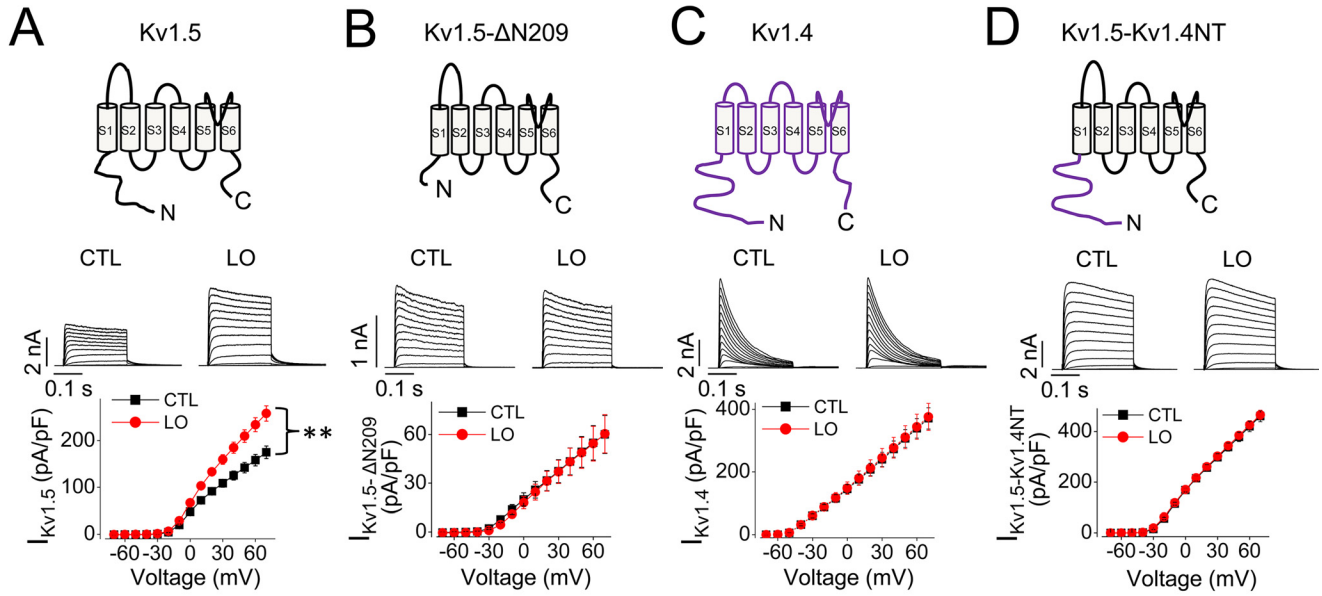

E

```
Kv1.5  MEIALVPLENGGAM----------------------------TVRGGDEARAGCGQATGGELQCPPTAGLSDGPKEPAPK 52
Kv1.4  MEVAMVSAESSGCNSHMPYGYAAQARARERERLAHSRAAAAAAVAAATAAVEGSGGSGGGSHHHHQSRGACTSHDPQSSR 80

Kv1.5  GRGA---QR----DADSGVRPLPPLPDPGVRPLPPLP------EELPRPRRPPPED--EEEEGDPGL----------GT 106
Kv1.4  GSRRRRRQRSEKKKAHYRQSSFPH-----CSDLMPSGSEEKILRELSEEEEDEEEEEEEEEEGRFYYSEDDHGDECSYTD 155

Kv1.5  VEDQ---ALG----TASLHHQRVHINISGLRFETQLGTLAQFPNTLLGDPAKRLRYFDPLRNEYFFDRNRPSFDGILYYY 179
Kv1.4  LLPQDEGGGGYSSVRYSDCCERVVINVSGLRFETQMKTLAQFPETLLGDPEKRTQYFDPLRNEYFFDRNRPSFDAILYYY 235

Kv1.5  QSGGRLRRPVNVSLDVFADEIRFYQLGDEAMERFREDEGFIKEE-EKPLPRNEFQRQVWLIFEYPESSG 247
Kv1.4  QSGGRLKRPVNVPFDIFTEEVKFYQLGEEALLKFREDEGFVREEEDRALPENEFKKQIWLLFEYPESSS 304
```

Figure 6. The N terminus is involved in LO-mediated increase in $I_{Kv1.5}$. *A*, LO treatment for 30 min increased $I_{Kv1.5}$. Schematic illustration of WT Kv1.5 channel (*top*) and representative current traces (*middle*) are depicted above the summarized I-V relationships (*bottom*). CTL, $n = 47$; LO, $n = 31$; **, $p < 0.01$ at 20 mV and above (same set of data shown in Figs. 2*B* and 4 for Kv1.5). *B*, N terminus truncation mutant ΔN209 abolished LO-induced increase in $I_{Kv1.5}$. Schematic illustration of Kv1.5-ΔN209 mutant (*top*) and representative current traces (*middle*) are depicted above the summarized I-V relationships (*bottom*). CTL, $n = 13$; LO, $n = 11$. *C*, LO treatment for 30 min had no effects on $I_{Kv1.4}$. Schematic illustration of WT Kv1.4 channel (*top*) and representative current traces (*middle*) are depicted above the summarized I-V relationships (*bottom*). CTL, $n = 43$; LO, $n = 46$ (same set of data shown in Fig. 4 for Kv1.4); *D*, replacement of the N terminus of Kv1.5 with the N terminus of Kv1.4 prevented LO-induced increase in $I_{Kv1.5}$. Schematic illustration of Kv1.5–Kv1.4NT mutant (*top*) and representative current traces (*bottom*) are depicted above the summarized I-V relationships (*bottom*). CTL, $n = 32$; LO, $n = 30$. *E*, amino acid sequence alignment of the N termini of Kv1.5 (1–247, UniProt: P22460) and Kv1.4 (1–304, UniProt: P22459), with Kv1.5 SH3-binding motifs shown in *blue*.

were recorded in normal, isotonic Tyrode solution. This LO treatment increased $I_{Kv1.5}$ (Fig. 2). However, LO treatment during whole-cell voltage clamp recordings did not affect $I_{Kv1.5}$ (data not shown). These observations are consistent with our finding that intracellular Src signaling (Figs. 6 and 7) and associated protein trafficking (Fig. 8) are involved in LO-mediated $I_{Kv1.5}$ increase. The disturbance of the intercellular environment by the whole-cell patch clamp configuration (32) likely prevented the LO treatment–mediated $I_{Kv1.5}$ increase.

Detecting mechanical forces exerted on cells requires a sensor. Transmembrane cytoskeletal proteins are able to detect changes in membrane lipid structure and are involved in transduction of mechanical force (33–35). As well, proline (Pro) residues, which provide rigidity to the polypeptide chain, are proposed to play important structural and functional roles for channel activity (19–22). This led to our investigation of the uniquely long and proline-rich extracellular S1–S2 linker of Kv1.5 channels. The LO-mediated increase in $I_{Kv1.5}$ was abolished by cleavage of the S1–S2 linker using PK treatment, replacement of 12 nonconserved prolines in the S1–S2 linker with alanines, or deletion of residues 282–300 from the S1–S2 linker (Fig. 5, *B–D*). Furthermore, the *N*-linked glycosylation is located in the middle (Asn-299) of the extracellular S1–S2 linker. Our results showed that inhibition of glycosylation abolished LO-mediated increase in $I_{Kv1.5}$ (Fig. 5*E*). Thus, the bulky, extracellular exposed glycan also plays a role in sensing mechanical forces. Overall, our results revealed a novel role of the extracellular S1–S2 linker as a sensor, capable of converting membrane stretch into biochemical signals that affect channel function. In line with this, the atypical structure of the Kv1.5 S1–S2 linker provides an explanation for how mechanical stretch is specific to the Kv1.5 channel among various Kv channels examined (Fig. 4).

Our results also revealed that the N terminus is involved in the LO-mediated increase in $I_{Kv1.5}$ (Fig. 6). The current of the N-terminal truncation mutant, ΔN209, was unresponsive to

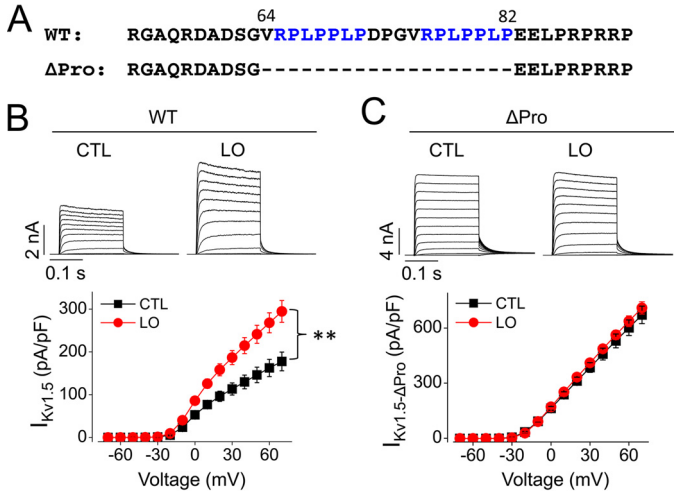

Figure 7. Removal of Src-binding sites abolishes LO-mediated increase in $I_{Kv1.5}$. *A,* amino acid sequences showing the two consensus SH3–binding motifs (RPLPPLP, shown in *blue*) in the N terminus of Kv1.5 as well as the mutant Kv1.5-ΔPro, in which amino acids 64–82 were removed. *B,* effects of LO treatment on WT $I_{Kv1.5}$. CTL, $n = 36$; LO, $n = 27$; **, $p < 0.01$ at 20 mV and above. *C,* removal of the Src-binding sites in Kv1.5 prevented LO-induced increase in $I_{Kv1.5}$. Representative current traces (*top*) are depicted above the summarized I-V relationships (*bottom*). CTL, $n = 26$; LO, $n = 28$.

LO treatment (Fig. 6*B*). The involvement of the Kv1.5 N terminus was further determined by creating a Kv1.5 mutant channel Kv1.5–Kv1.4NT, in which the N terminus of Kv1.5 was replaced by the N terminus of Kv1.4, a Kv channel that is unaffected by LO treatment (Fig. 6*C*). Kv1.5–Kv1.4NT channels were not affected by LO treatment (Fig. 6*D*). The N terminus of the Kv1.5 channel contains a proline-rich motif for binding of Src kinase, and the Src-channel interaction leads to a suppression of $I_{Kv1.5}$ (23). Endogenous Src exists in HEK cells and cardiac myocytes (23, 25, 26), and association between Kv1.5 and native Src has been demonstrated in human myocardium tissue lysates (23). Our results revealed that inhibition of Src tyrosine kinase by PP1 increased $I_{Kv1.5}$ to an extent similar to LO treatment. Furthermore, after PP1 pretreatment, LO treatment no longer increased $I_{Kv1.5}$ (Fig. 8*C*). To confirm the role of Src tyrosine kinase binding in mechanical stretch, we created a Kv1.5 mutant channel, Kv1.5-ΔPro, by deleting the SH3 domain–binding motifs within the N terminus (Fig. 7). Removal of the Kv1.5 channel Src-binding sites led to an increase in $I_{Kv1.5}$ (note the current amplitude between Fig. 7, *B* and *C*), consistent with the notion that Kv1.5 channel activity is constitutively inhibited by endogenous Src kinases. Deletion of Src-binding sites abolished the LO-mediated current increase (Fig. 7*C*). These results suggest that LO treatment is likely to increase $I_{Kv1.5}$ by relieving the constitutive inhibition caused by endogenous Src tyrosine kinase.

We then investigated how LO treatment affects the interaction of the N terminus with Src kinase. Our results revealed that the N terminus communicates with the S1–S2 linker. Although PK completely cleaved the mature protein of WT Kv1.5 channels, it could not cleave the mature protein of the N-terminal truncation mutant, Kv1.5 ΔN209 (Fig. 9). The S1–S2 linker of Kv1.5 is exposed extracellularly, whereas the N terminus is localized intracellularly. Thus, the resistance of Kv1.5 ΔN209 to PK cleavage provides direct evidence that shortening the intracellularly localized N terminus affects the conformation of the extracellularly localized S1–S2 linker, preventing cleavage by PK. Inversely, we believe that a change in the S1–S2 linker induced by mechanical forces may lead to conformational alteration of the N terminus. Such a change may cause Src dissociation and relief of tonic inhibition of the channel, leading to an increase in $I_{Kv1.5}$. It remains to be elucidated which and how extracellular matrix molecules are coupled to the S1–S2 linker of Kv1.5 channels to affect channel function. Nonetheless, our study raised the possibility that a mechanical stimulus can act on the extracellular S1–S2 linker that allosterically couples to an intracellular event (*e.g.* Src dissociation and relief of inhibition). Because Kv1.5 plays an important role in atrial repolarization (1, 2) and atrial stretch is associated with atrial fibrillation (36), the role of Kv1.5 in this association warrants further investigation.

It is not well-understood how Src binding to the channel causes an inhibition of channel currents. Our results showed that the LO-induced increase in $I_{Kv1.5}$ was not associated with a change in the activation-voltage relationship of the channel (Fig. 2*B*). Boycott *et al.* (15) reported that shear stress triggers plasma membrane insertion of Kv1.5 channels from intracellular compartments in atrial myocytes. Consistently, our results showed that LO and PP1 treatment increased the cell surface Kv1.5 expression without affecting the total amount of Kv1.5 proteins from whole-cell lysate (Fig. 8, *A* and *B*). This result suggests that disruption of the endogenous Src-channel interaction enhances the longevity of Kv1.5 channels on the plasma membrane, leading to accumulated membrane expression and increased $I_{Kv1.5}$.

In summary, by subjecting cells to centrifugation and hypotonic solution, our study revealed mechanical stretch as a novel pathway for Kv1.5 channel regulation. Mechanical stretch is detected by the S1–S2 linker of the Kv1.5 channel, which communicates with the N terminus, relieving Src-mediated tonic inhibition, leading to an increase in $I_{Kv1.5}$.

Experimental procedures

Molecular biology

WT human Kv1.5 cDNA was provided by Dr. Michael Tamkun (Colorado State University, Fort Collins, CO). Human ether-a-go-go related gene (hERG) cDNA was provided by Dr. Gail Robertson (University of Wisconsin-Madison). Human ether-a-go-go gene (hEAG) was provided by Dr. Luis Pardo (Max-Planck Institute of Experimental Medicine, Göttingen, Germany). Human KCNQ1 and KCNE1 cDNAs were provided by Dr. Michael Sanguinetti (University of Utah, Salt Lake City, UT). Human Kv4.3 was provided by Gui-Rong Li (University of Hong Kong, Hong Kong, China). Kv1.4 cDNA was purchased from GenScript. Mutations in Kv1.5 channel, including Kv1.5-ΔN209 (deletion of amino acids 1–209), Kv1.5-Δ282–300 (deletion of amino acids 282–300 in S1–S2 linker), Kv1.5-ΔPro (deletion of amino acids 64–82 which contains Src-binding motifs), Kv1.5–12PA (mutating all 12 prolines to alanines in the S1–S2 linker), and Kv1.5–Kv1.4NT (the N terminus of Kv1.5 replaced by the N terminus of Kv1.4) were generated by PCR cloning of the corresponding constructs from WT Kv1.5 and

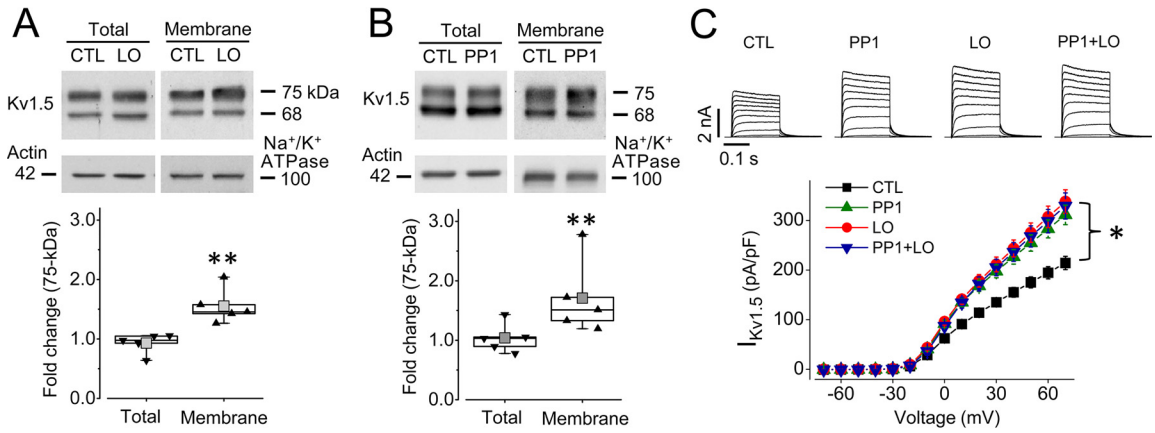

Figure 8. Effects of LO-treatment and Src inhibitor PP1 on Kv1.5 expression and function. *A*, LO treatment did not affect the total amount of Kv1.5 proteins but increased the cell surface mature channel expression. The density of the 75-kDa band in LO-treated cells was normalized to that of control cells in the same gel and shown in the scatter plots ($n = 5$). *B*, PP1 treatment did not affect the total amount of Kv1.5 proteins but increased the cell surface mature channel expression. The density of the 75-kDa band in PP1-treated cells was normalized to that of control cells in the same gel and shown in the scatter plot ($n = 5$). For *A* and *B*, *boxes* represent interquartile ranges, *horizontal lines* represent medians, *whiskers* represent 5–95% ranges, and *gray boxes* represent means. **, $p < 0.01$ *versus* CTL. *C*, Src inhibitor PP1 treatment increased $I_{Kv1.5}$ and prevented LO-mediated increase in $I_{Kv1.5}$. Representative current traces (*top*) are depicted above the summarized I-V relationships (*bottom*). CTL, $n = 32$; PP1, $n = 35$; LO, $n = 26$; PP1+LO, $n = 28$. *, $p < 0.05$ at 20 mV and above, compared with control (CTL). There was no significant difference among PP1, LO, and PP1+LO groups.

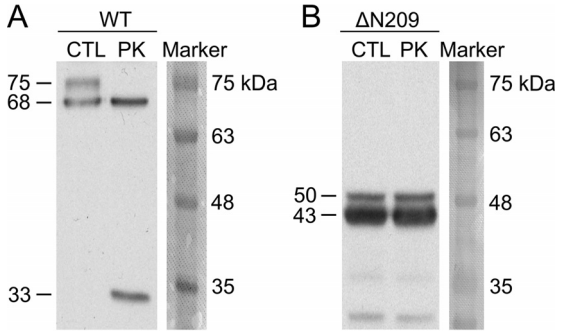

Figure 9. The Kv1.5 S1–S2 linker communicates with the N terminus in a conformational manner. Truncation of N terminus altered the susceptibility of the S1–S2 linker to PK cleavage. WT Kv1.5 displays 75-kDa and 68-kDa bands on Western blot analysis. The 75-kDa band represents the mature, fully glycosylated channel protein in the plasma membrane, whereas the 68-kDa band represents the immature channel protein inside the cell. ΔN209 Kv1.5 also presents as two bands; the 50-kDa band represents mature protein in the plasma membrane, the 43-kDa band represents immature protein inside the cell. Although PK completely cleaved the mature (cell surface) channel proteins of WT Kv1.5, it failed to cleave the mature (cell surface) channel proteins of ΔN209 Kv1.5 ($n = 6$).

Kv1.4 template and using BamH1 and EcoR1 restriction enzymes in the pcDNA3 vector. All sequencings were verified by GENEWIZ (South Plainfield, NJ). Human embryonic kidney (HEK) 293 cell lines stably expressing Kv1.5, Kv1.4, Kv4.3, KCNQ1 (Kv7.1) + KCNE1, hEAG (Kv10.1), hERG (Kv11.1), or each of the mutant Kv1.5 channels were created using Lipofectamine 2000 to transfect the respective plasmid into HEK 293 cells, followed by G418 for selection (1 mg/ml) and maintenance (0.4 mg/ml). Cells were cultured in MEM supplemented with 10% FBS, 1 mM sodium pyruvate, and 1% nonessential amino acids (Thermo Fisher Scientific).

Neonatal rat ventricular myocyte isolation and culture

Neonatal rat experiments were approved by the Queen's University Animal Care Committee. Ventricles of Sprague-Dawley rats of either sex at 1 day old were used to isolate ventricular myocytes using enzymatic dissociation (37). Isolated ventricular myocytes were initially cultured in 10% FBS-containing DF medium for 45 min to allow fibroblasts to adhere to the bottom of the plate. Unadhered ventricular myocytes were then transferred to culture plates with glass coverslips and cultured overnight. Kv1.5 and GFP plasmids at a 4:1 ratio were transfected to ventricular myocytes using Lipofectamine 2000. Twenty-four h after transfection, GFP-positive cells were used to record $I_{Kv1.5}$ using the same voltage protocols and solutions as in HEK cells.

Mechanical stretch induced by centrifugation and LO treatment

To induce mechanical stretch, Kv1.5-HEK cells were detached from plates with trypsin, placed in tubes, and centrifuged at 70 × *g* for 5 min. The centrifuged cells were then resuspended and transferred for patch clamp recordings. Control cells were collected in the same way, but without centrifugation (detached with trypsin and placed in tubes). We also induced mechanical stretch in Kv1.5-HEK cells with LO medium culture for 30 min. LO media were created by diluting standard cell culture medium (MEM with 10% FBS) with purified water at a 2:1 ratio, decreasing the osmolarity of the medium from 315 to 211 mOsm/liter (33% reduction).

Extracellular cleavage of cell surface proteins

To cleave the extracellularly localized S1–S2 linker of Kv1.5 channels, the cells were treated with the serine protease PK (200 μg/ml in MEM) for 20 min at 37 °C. PBS containing 6 mM PMSF and 25 mM EDTA was then used to terminate the reaction. Biochemical and electrophysiological experiments were performed to detect the channel protein expression and current. Kv1.5-HEK cells treated with 250 μg/ml trypsin in PBS for 20 min at 37 °C were used as control.

Western blot analysis

Whole-cell protein lysates were used for Western blot analysis using the procedure described previously (5, 6). Cells were

washed and collected with ice-cold PBS and centrifuged for 4 min at 100 × *g*. Cell pellets were then lysed in ice-cold lysis buffer containing 1 mM PMSF and 1% protease inhibitor mixture using sonification. Next, the cell lysates were centrifuged for 10 min at 10,000 × *g*, and supernatants containing proteins were collected. A protein assay kit (Bio-Rad) was used to determine protein concentrations. To create 0.3 μg/μl protein samples the appropriate amounts of double-distilled water and loading buffer containing 5% β-mercaptoethanol were added to the protein. Proteins samples of 15 μg were loaded and separated on 8% SDS-polyacrylamide gels and transferred onto PVDF membranes. To prevent nonspecific protein interactions, membranes were blocked with 5% nonfat skim milk and 0.1% Tween 20 in TBS for 1 h at room temperature. The blots were incubated with a C terminus–specific rabbit anti-Kv1.5 primary antibody (APC-004, Alomone) for 1 h at room temperature and then with goat anti-rabbit HRP-conjugated secondary antibody for 1 h. The blots were visualized with Fuji X-ray films (Fujifilm, Tokyo, Japan) using an enhanced chemiluminescence detection kit (GE Healthcare).

Isolation of cell surface proteins

Cell membrane proteins were isolated using biotinylation method with a Cell Surface Protein Isolation Kit (89881, Thermo Fisher Scientific). Specifically, cells at 90% confluence on 100-mm plates were treated with a membrane-impermeable thiol-cleavable amine-reactive biotinylation reagent, Sulfo-NHS-SS-biotin (250 μg/ml) for 30 min at 4 °C. Quenching solution was then added, and cells were lysed. After centrifugation at 10,000 × *g* for 2 min at 4 °C, biotin-labeled proteins were isolated using NeutrAvidin agarose columns and eluted with SDS-polyacrylamide sample buffer containing DTT. The isolated cell surface proteins were analyzed using Western blot analysis to detect Kv1.5 membrane expression. To ensure equal loadings, Na^+/K^+ ATPase expression was detected with a mouse anti-Na^+/K^+-ATPase α-1 antibody and a horse anti-mouse HRP-conjugated secondary antibody.

Electrophysiological recordings

All currents were recorded using whole-cell voltage clamp method. Cells collected were allowed to settle on the bottom of a 0.5 ml perfusion chamber in bath solution. The glass pipettes were pulled using thin-walled borosilicate glass (World Precision Instruments, Sarasota, FL). The pipettes had inner diameters of ~1.5 μm and resistances of 2 MΩ when filled with solution. Series resistance (Rs) was compensated by 80%, and leak subtraction was not used. An Axopatch 200B amplifier and pCLAMP10 (Molecular Devices, San Jose, CA) were used for data acquisition and analysis. Data were sampled at 20 kHz and filtered at 5 kHz. The bath solution contained (in mM) 135 NaCl, 5 KCl, 10 HEPES, 10 glucose, 1 $MgCl_2$, and 2 $CaCl_2$ (pH 7.4 with NaOH). The pipette solution contained (in mM) 135 KCl, 5 EGTA, 5 MgATP, and 10 HEPES (pH 7.2 with KOH). For whole-cell voltage clamp recordings, currents were elicited from a holding potential of −80 mV by depolarizing steps to voltages between −70 and +70 mV in 10-mV increments. The membrane was then clamped to −50 mV (−30 mV for Kv1.5) prior to returning to the holding potential. Current amplitudes were normalized to the cell capacitances and expressed as current density (pA/pF). For current-voltage relationships of all channels, current amplitudes upon depolarizing steps were measured and plotted against voltages. For the Kv1.5 activation curve, peak tail currents during the −30 mV repolarizing step were measured, and plotted against the depolarizing voltages; the tail current-voltage relationships were fitted to the Boltzmann equation to obtain half-activation voltages ($V_{1/2}$) and slope factors. Patch clamp experiments were performed at room temperature (22 ± 1 °C).

Live cell microscopy

WT Kv1.5-HEK cells were cultured on glass-bottom plates (35 mm) (World Precision Instruments, Sarasota, FL). Before and after culture with LO medium for 30 min at 37 °C, cell images were obtained using a 63× oil objective on a Zeiss Z.1 AxioObserver inverted microscope (Zeiss, Oberkochen, Germany). To quantify cell size, Zeiss AxioVision software was used.

Reagents and antibodies

A C terminus–specific rabbit anti-Kv1.5 antibody (APC-004) was purchased from Alomone Labs (Jerusalem, Israel). A mouse anti-Na^+/K^+-ATPase α-1 (sc-21712) primary antibody was purchased from Santa Cruz Biotechnology (Dallas, TX). Horse anti-mouse (7076) and goat anti-rabbit (7074) HRP-conjugated secondary antibodies were purchased from Cell Signaling Technology (Danvers, MA). MEM, FBS, trypsin, sodium pyruvate, minimal essential amino acids, Lipofectamine 2000, and Opti-MEM were purchased from Thermo Fisher Scientific. G418, PMSF, protease inhibitor mixture, β-mercaptoethanol, proteinase K, Triton X-100, BSA, and all chemicals/electrolytes used in the patch clamp experiments were obtained from Sigma-Aldrich. The BLUeye Prestained Protein Ladder (GeneDirex) was purchased from FroggaBio (Toronto, Ontario, Canada). An enhanced chemiluminescence detection kit was purchased from GE Healthcare. X-ray films were from Fujifilm (Tokyo, Japan).

Statistical analysis

All data are expressed as the mean ± S.E. For experiments with multiple groups, a two-way analysis of variance with Bonferroni post hoc test was used. For experiments between two groups, a two-tailed unpaired Student's *t* test was used, except for Fig. 2*A* where a two-tailed paired Student's *t* test was used. A p value ≤ 0.05 was considered statistically significant.

Data availability

All the data are in the manuscript.

Author contributions—A. O. M., T. W., W. L., and J. G. data curation; A. O. M., T. W., W. L., and J. G. formal analysis; A. O. M., T. W., and S. Z. investigation; A. O. M. and T. W. writing-original draft; A. O. M., T. W., W. L., J. G., and S. Z. writing-review and editing; S. Z. conceptualization; S. Z. supervision; S. Z. funding acquisition; S. Z. validation; S. Z. project administration.

References

1. Fedida, D., Wible, B., Wang, Z., Fermini, B., Faust, F., Nattel, S., and Brown, A. M. (1993) Identity of a novel delayed rectifier current from human heart with a cloned K^+ channel current. *Circ. Res.* **73,** 210–216 CrossRef Medline
2. Wang, Z., Fermini, B., and Nattel, S. (1993) Sustained depolarization-induced outward current in human atrial myocytes: Evidence for a novel delayed rectifier K^+ current similar to Kv1.5 cloned channel currents. *Circ. Res.* **73,** 1061–1076 CrossRef Medline
3. Archer, S. L., Souil, E., Dinh-Xuan, A. T., Schremmer, B., Mercier, J. C., El Yaagoubi, A., Nguyen-Huu, L., Reeve, H. L., and Hampl, V. (1998) Molecular identification of the role of voltage-gated K^+ channels, Kv1.5 and Kv2.1, in hypoxic pulmonary vasoconstriction and control of resting membrane potential in rat pulmonary artery myocytes. *J. Clin. Invest.* **101,** 2319–2330 CrossRef Medline
4. Ohanyan, V., Yin, L., Bardakjian, R., Kolz, C., Enrick, M., Hakobyan, T., Kmetz, J., Bratz, I., Luli, J., Nagane, M., Khan, N., Hou, H., Kuppusamy, P., Graham, J., Fu, F. K., *et al.* (2015) Requisite role of Kv1.5 channels in coronary metabolic dilation. *Circ. Res.* **117,** 612–621 CrossRef Medline
5. Hogan-Cann, A., Li, W., Guo, J., Yang, T., and Zhang, S. (2016) Proteolytic cleavage in the S1-S2 linker of the Kv1.5 channel does not affect channel function. *Biochim. Biophys. Acta* **1858,** 1082–1090 CrossRef Medline
6. Lamothe, S. M., Hogan-Cann, A. E., Li, W., Guo, J., Yang, T., Tschirhart, J. N., and Zhang, S. (2018) The N terminus and transmembrane segment S1 of Kv1.5 can coassemble with the rest of the channel independently of the S1-S2 linkage. *J. Biol. Chem.* **293,** 15347–15358 CrossRef Medline
7. Yang, T., Yang, P., Roden, D. M., and Darbar, D. (2010) Novel KCNA5 mutation implicates tyrosine kinase signaling in human atrial fibrillation. *Heart Rhythm* **7,** 1246–1252 CrossRef Medline
8. Christophersen, I. E., Olesen, M. S., Liang, B., Andersen, M. N., Larsen, A. P., Nielsen, J. B., Haunsø, S., Olesen, S. P., Tveit, A., Svendsen, J. H., and Schmitt, N. (2013) Genetic variation in KCNA5: Impact on the atrial-specific potassium current I_{Kur} in patients with lone atrial fibrillation. *Eur. Heart J.* **34,** 1517–1525 CrossRef Medline
9. Go, A. S., Hylek, E. M., Phillips, K. A., Chang, Y., Henault, L. E., Selby, J. V., and Singer, D. E. (2001) Prevalence of diagnosed atrial fibrillation in adults: National implications for rhythm management and stroke prevention. The AnTicoagulation and Risk Factors in Atrial Fibrillation (ATRIA) Study. *JAMA* **285,** 2370–2375 CrossRef Medline
10. Anter, E., Jessup, M., and Callans, D. J. (2009) Atrial fibrillation and heart failure: Treatment considerations for a dual epidemic. *Circulation* **119,** 2516–2525 CrossRef Medline
11. Dzeshka, M. S., Shantsila, A., Shantsila, E., and Lip, G. Y. H. (2017) Atrial fibrillation and hypertension. *Hypertension* **70,** 854–861 CrossRef Medline
12. Noubiap, J. J., Bigna, J. J., Agbor, V. N., Mbanga, C., Ndoadoumgue, A. L., Nkeck, J. R., Kamguia, A., Nyaga, U. F., and Ntusi, N. A. B. (2019) Meta-analysis of atrial fibrillation in patients with various cardiomyopathies. *Am. J. Cardiol.* **124,** 262–269 CrossRef Medline
13. Peyronnet, R., Nerbonne, J. M., and Kohl, P. (2016) Cardiac mechano-gated ion channels and arrhythmias. *Circ. Res.* **118,** 311–329 CrossRef Medline
14. Guo, W., Kamiya, K., Kada, K., Kodama, I., and Toyama, J. (1998) Regulation of cardiac Kv1.5 K^+ channel expression by cardiac fibroblasts and mechanical load in cultured newborn rat ventricular myocytes. *J. Mol. Cell. Cardiol.* **30,** 157–166 CrossRef Medline
15. Boycott, H. E., Barbier, C. S., Eichel, C. A., Costa, K. D., Martins, R. P., Louault, F., Dilanian, G., Coulombe, A., Hatem, S. N., and Balse, E. (2013) Shear stress triggers insertion of voltage-gated potassium channels from intracellular compartments in atrial myocytes. *Proc. Natl. Acad. Sci. U.S.A.* **110,** E3955–E3964 CrossRef Medline
16. Montrose-Rafizadeh, C., and Guggino, W. B. (1990) Cell volume regulation in the nephron. *Annu. Rev. Physiol* **52,** 761–772 CrossRef Medline
17. Chan, H. C., and Nelson, D. J. (1992) Chloride-dependent cation conductance activated during cellular shrinkage. *Science* **257,** 669–671 CrossRef Medline
18. Volk, T., Frömter, E., and Korbmacher, C. (1995) Hypertonicity activates nonselective cation channels in mouse cortical collecting duct cells. *Proc. Natl. Acad. Sci. U.S.A.* **92,** 8478–8482 CrossRef Medline
19. Wess, J., Nanavati, S., Vogel, Z., and Maggio, R. (1993) Functional role of proline and tryptophan residues highly conserved among G protein-coupled receptors studied by mutational analysis of the m3 muscarinic receptor. *EMBO J.* **12,** 331–338 CrossRef Medline
20. Hong, S., Ryu, K. S., Oh, M. S., Ji, I., and Ji, T. H. (1997) Roles of transmembrane prolines and proline-induced kinks of the lutropin/choriogonadotropin receptor. *J. Biol. Chem.* **272,** 4166–4171 CrossRef Medline
21. Kaduk, C., Duclohier, H., Dathe, M., Wenschuh, H., Beyermann, M., Molle, G., and Bienert, M. (1997) Influence of proline position upon the ion channel activity of alamethicin. *Biophys. J.* **72,** 2151–2159 CrossRef Medline
22. Bett, G. C., Lis, A., Guo, H., Liu, M., Zhou, Q., and Rasmusson, R. L. (2012) Interaction of the S6 proline hinge with N-type and C-type inactivation in Kv1.4 channels. *Biophys. J.* **103,** 1440–1450 CrossRef Medline
23. Holmes, T. C., Fadool, D. A., Ren, R., and Levitan, I. B. (1996) Association of Src tyrosine kinase with a human potassium channel mediated by SH3 domain. *Science* **274,** 2089–2091 CrossRef Medline
24. Yu, H., Chen, J. K., Feng, S., Dalgarno, D. C., Brauer, A. W., and Schreiber, S. L. (1994) Structural basis for the binding of proline-rich peptides to SH3 domains. *Cell* **76,** 933–945 CrossRef Medline
25. Holmes, T. C., Fadool, D. A., and Levitan, I. B. (1996) Tyrosine phosphorylation of the Kv1.3 potassium channel. *J. Neurosci.* **16,** 1581–1590 CrossRef Medline
26. Torsoni, A. S., Constancio, S. S., Nadruz, W., Jr., Hanks, S. K., and Franchini, K. G. (2003) Focal adhesion kinase is activated and mediates the early hypertrophic response to stretch in cardiac myocytes. *Circ. Res.* **93,** 140–147 CrossRef Medline
27. Hanke, J. H., Gardner, J. P., Dow, R. L., Changelian, P. S., Brissette, W. H., Weringer, E. J., Pollok, B. A., and Connelly, P. A. (1996) Discovery of a novel, potent, and Src family selective tyrosine kinase inhibitor. Study of Lck- and FynT-dependent T cell activation. *J. Biol. Chem.* **271,** 695–701 CrossRef Medline
28. Yang, F., and Zheng, J. (2014) High temperature sensitivity is intrinsic to voltage-gated potassium channels. *Elife* **3,** e03255 Medline
29. Gomis, A., Soriano, S., Belmonte, C., and Viana, F. (2008) Hypoosmotic- and pressure-induced membrane stretch activate TRPC5 channels. *J. Physiol.* **586,** 5633–5649 CrossRef Medline
30. Linz, P., and Veelken, R. (2002) Serotonin 5-HT(3) receptors on mechanosensitive neurons with cardiac afferents. *Am. J. Physiol. Heart Circ. Physiol.* **282,** H1828–H1835 CrossRef Medline
31. Schmidt, D., del Mármol, J., and MacKinnon, R. (2012) Mechanistic basis for low threshold mechanosensitivity in voltage-dependent K^+ channels. *Proc. Natl. Acad. Sci. U.S.A.* **109,** 10352–10357 CrossRef Medline
32. Zhang, S., Hiraoka, M., and Hirano, Y. (1998) Effects of α1-adrenergic stimulation on L-type Ca^{2+} current in rat ventricular myocytes. *J. Mol. Cell Cardiol.* **30,** 1955–1965 CrossRef Medline
33. Fonseca, P. M., Inoue, R. Y., Kobarg, C. B., Crosara-Alberto, D. P., Kobarg, J., and Franchini, K. G. (2005) Targeting to C-terminal myosin heavy chain may explain mechanotransduction involving focal adhesion kinase in cardiac myocytes. *Circ. Res.* **96,** 73–81 CrossRef Medline
34. Han, B., Bai, X. H., Lodyga, M., Xu, J., Yang, B. B., Keshavjee, S., Post, M., and Liu, M. (2004) Conversion of mechanical force into biochemical signaling. *J. Biol. Chem.* **279,** 54793–54801 CrossRef Medline
35. Katsumi, A., Naoe, T., Matsushita, T., Kaibuchi, K., and Schwartz, M. A. (2005) Integrin activation and matrix binding mediate cellular responses to mechanical stretch. *J. Biol. Chem.* **280,** 16546–16549 CrossRef Medline
36. De Jong, A. M., Maass, A. H., Oberdorf-Maass, S. U., Van Veldhuisen, D. J., Van Gilst, W. H., and Van Gelder, I. C. (2011) Mechanisms of atrial structural changes caused by stretch occurring before and during early atrial fibrillation. *Cardiovasc. Res.* **89,** 754–765 CrossRef Medline
37. Tschirhart, J. N., Li, W., Guo, J., and Zhang, S. (2019) Blockade of the human ether a-go-go related gene (hERG) potassium channel by fentanyl. *Mol. Pharmacol.* **95,** 386–397 CrossRef Medline